Draft
Pending technical review

PAVEMENT SUBGRADE PERFORMANCE STUDY

Test Section 708

Subgrade AASHTO soil type A-6 at wet of optimum (19%)

By

Dr. Vincent Janoo[1]
Mr. Edel Cortez[1]

Subgrade Moisture Content	AASHTO Soil Type			
	A-2-4	A-4	A-6	A-7-6
M1	Optimum 10 % TS 701	Optimum 17 % TS 702	Optimum 16 % TS 709	Optimum TBD*
M2	12 % TS 707	19 % TS 704	**19 % TS 708**	TBD
M3	15 % TS 703	23 % TS 705	22 % TS 706	TBD

1. U.S. Army Cold Regions Research and Engineering Laboratory, 72 Lyme Road, Hanover, New Hampshire 03755, United States

EXECUTIVE SUMMARY

This is one of a series of reports on the subgrade performance research study. The hypothesis for this study is that the failure criterion depends on the subgrade soil type and the in-situ moisture content. Many of the current mechanistic design procedures incorporate the results from AASHTO Road Tests conducted in the late fifties. However, the AASHTO Road Tests were all conducted on only one soil type (AASHTO type A-6). The tests results reflect the combined effect of traffic loads and seasonal variations. Applying failure criteria based on the AASHTO Road Tests to other soil types, at different moisture contents and different climates, creates much uncertainty.

In recent decades much progress has been achieved in computer technology, and new sensors allow reliable in-situ stress and strain measurements. The authors recognize the technological opportunities to develop more reliable pavement failure criteria that consider the effects of subgrade soil type and moisture condition.

Transportations agencies from several US states are contributing to a research initiative that will develop the basis for new pavement failure criteria that is adequate for the most common subgrade soil types found in the United State at various soil moisture contents. As part of the research program, four subgrade soils were selected for testing in the Frost Effects Research Facility (FERF). Each subgrade soil was to be constructed at three moisture contents, with one at or near optimum density and moisture content. The test sections consisted of 75 mm of asphalt concrete, 229 mm of crushed base and 3 m of the test subgrade soil type at pre-determined moisture content. The current test section was named Test Section 708. It represents the case of a subgrade soil AASHTO type A-6 at 19% gravimetric water content. For this soil type, the optimum moisture content is 16%. According to the Unified Soil Classification System, the subgrade soil was type CL (low liquid limit, clay).

Accelerated traffic was applied by means of a Heavy Vehicle Simulator (HVS). Each test window was subjected to one of various load levels. The traffic load was varied for each test window, ranging from 27 to 53 kN (6 to 12 kips). The load was applied through a dual truck tire assembly representing a half axle of a standard truck. Therefore, a 40-kN (9-kip) load is equivalent to an 80 kN (18-kip) load applied with a complete truck axle. The tire pressures were kept at 689 kPa (100 psi).

The test section was built inside the FERF testing facility; therefore, the moisture and temperature conditions were controlled. The test section contained six test windows. Each test window was approximately 6.0 m long and 1 m wide. Loading was applied unidirectionally at an average speed of 12 km/hr. The test windows were subjected to about 600 load repetitions per hour. The HVS applied traffic 23 hours per day. The remaining hour was used for maintenance.

Stress, strain, and surface rut measurements were taken periodically. Dynatest® stress sensors were embedded in a tri-axial arrangement in the subgrade at a depth of 76 mm (3 in.) from the top of the subgrade in all the test windows. Test windows 2 and 5 contained an additional tri-axial set of Dynatest stress cells at a depth of 230 mm (9 in.) from the top of the subgrade.

Dynamic and permanent strains in the base and subgrade were measured in all of the six test windows.

This report contains a description of the test section, construction, instrumentation, and pavement response to accelerated traffic.

TABLE OF CONTENTS

Illustrations

Tables

INTRODUCTION

As part of an international study on pavement subgrade performance, several full-scale test sections were constructed in the Frost Effects Research Facility (FERF) at the U.S. Army Engineer Research and Development Center, Cold Regions Research and Engineering Laboratory (CRREL) in Hanover, New Hampshire. The test sections were constructed using four subgrade soil types at three moisture contents. They were instrumented with stress cells, strain gages, moisture, and temperature sensors. The test sections were subjected to accelerated loading using the Heavy Vehicle Simulator (HVS). Pavement failure was defined at 12.5 mm (0.5 in.) surface rut depth. Surface rut depth measurements were taken periodically during the accelerated load tests. At the same time, subsurface stress and strain measurements were also taken. A detailed overview of the project can be found in Janoo et al. (2001). The test sections consisted of a 76-mm (3 in.) asphalt concrete (AC) layer, a 229-mm (9 in.) crushed gravel base and 3 m (10 ft) of subgrade soil. The tests were conducted indoors in the FERF at around 20°C. Provisions were made to maintain the temperature and moisture content as constant as possible.

This reports deals with the construction, accelerated traffic testing, and pavement response of Test Section 708. Test Section 708 corresponds to a subgrade soil AASHTO type A-6 conditioned at 19 percent moisture content.

DESCRIPTION OF THE TEST SECTION

The test section (Fig. 1) consists of a 76-mm (3-in.) asphalt concrete (AC) layer, a 229-mm (9-in) crushed gravel base course, and 3 m of AASHTO type A-6 subgrade soil conditioned to a gravimetric moisture content of 19%.

The test section was divided into six test windows. A test window is the area where traffic is applied. An effective test window was 0.91 m (3 ft) wide by 6.08 m (20 ft) long, excluding acceleration and deceleration areas. The thickness and material properties for all test windows were intended to be constant, but the traffic load was designed to vary for different test windows.

Each test window was instrumented with embedded sensors to measure in-situ stress, strain, moisture, and temperature at various locations within the pavement structure. Dynatest® stress cells were used to measure stress in the subgrade soil. Geokon® stress cells were embedded in the unbound base course. Strain was deducted from displacement measurements obtained by means of emu coil pairs. Vitel Hydra® sensors were used to record volumetric soil moisture content and temperature. Additionally, strings of thermocouples were used to record subgrade temperatures.

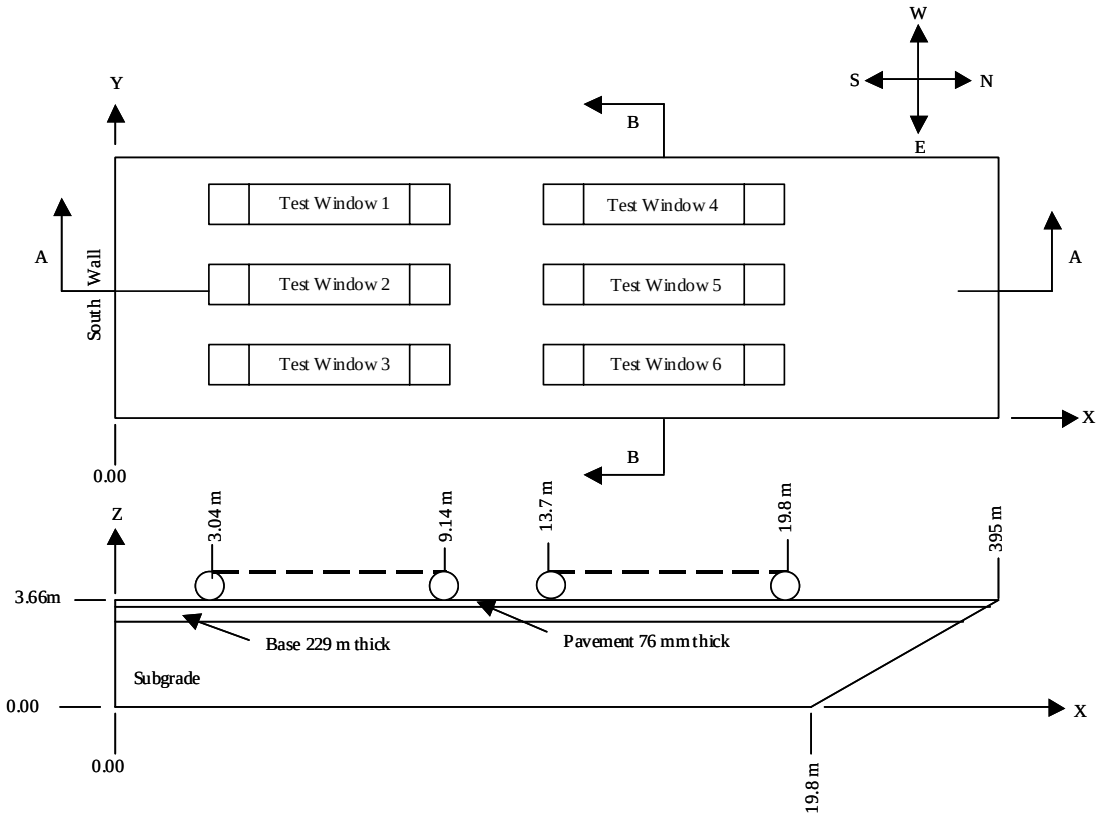

a. Plan view and longitudinal cross section.

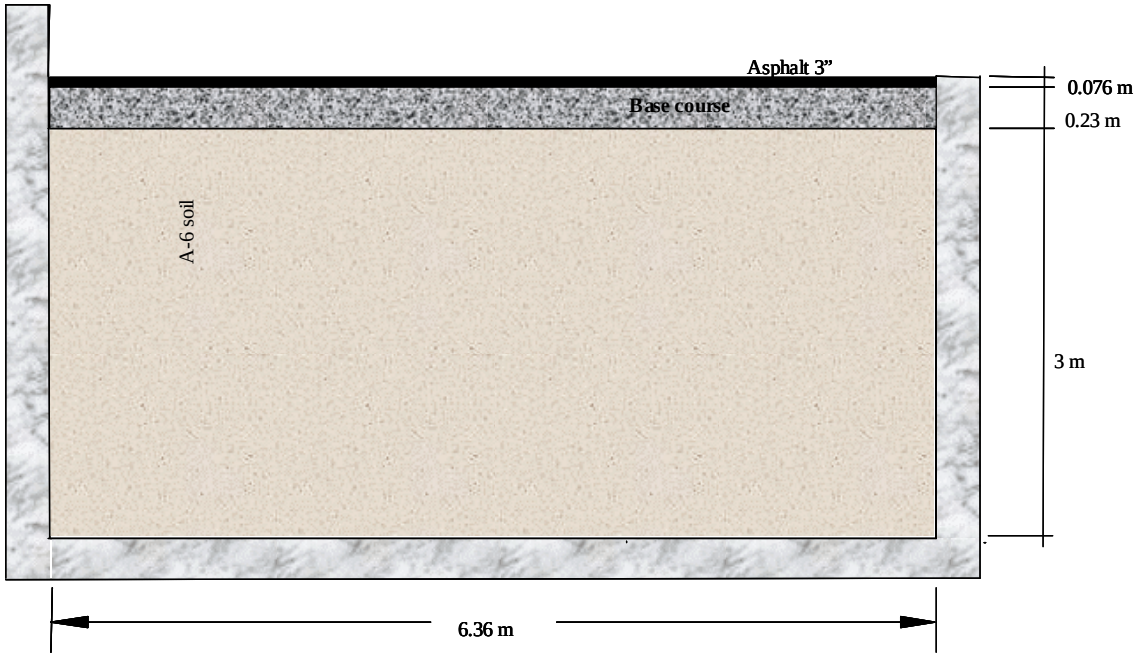

b. Transversal cross section.

Figure 1. Test section.

MATERIAL PROPERTIES

Laboratory tests were conducted on representative samples of the subgrade soil and the base course soil. The battery of tests included moisture and density, grain size distribution, specific gravity, liquid and plastic limits, and hydrometer tests.

Figure 2 shows grain size distributions for the subgrade soil and for the base course soil. The subgrade soil has approximately 92% passing the 0.074-mm sieve. The average liquid limit (LL) and plasticity index (PI) of the soil were 29 and 13% respectively. The average specific gravity of the subgrade soil was 2.70. According to the American Association of Highway and Transportation Officials (AASHTO) soil classification system, the subgrade soil was type A-6. According to the Unified Soil Classification System, the subgrade soil was type CL (low liquid limit, clay). See Table 1.

The base course material was made of unbound crushed stone. It was classified as an AASHTO type A-1 soil. According to the Unified Soil Classification System, the base course soil was type GP-GM (mix of poorly graded gravel and silty gravel). About 11% by weight of the base course soil particles passed through the sieve 0.074-mm (#200) sieve. The fines were classified as non-plastic.

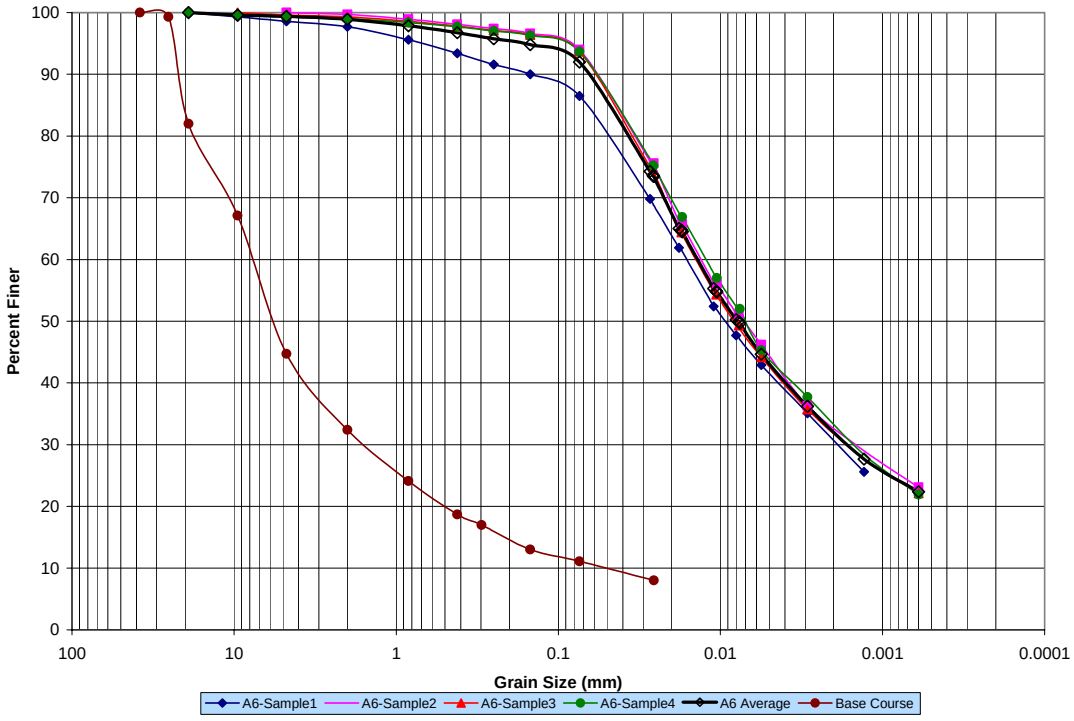

Figure 2. Grain size distribution for A-6 subgrade soil and base course

Laboratory tests were conducted to determine the optimum moisture content and maximum density for the base course and subgrade soils using the AASHTO test procedure, *The Moisture-Density Relations of Soils Using a 5.5 lb (2.5 kg) Rammer and a 12 in. (305 mm) Drop* (T 99-90). Samples were collected from various parts of the stockpile

for the test and the results from these tests are shown in Figure 3. The optimum density and moisture content was 1791 kg/m^3 (111.8 pcf) and 16 % respectively.

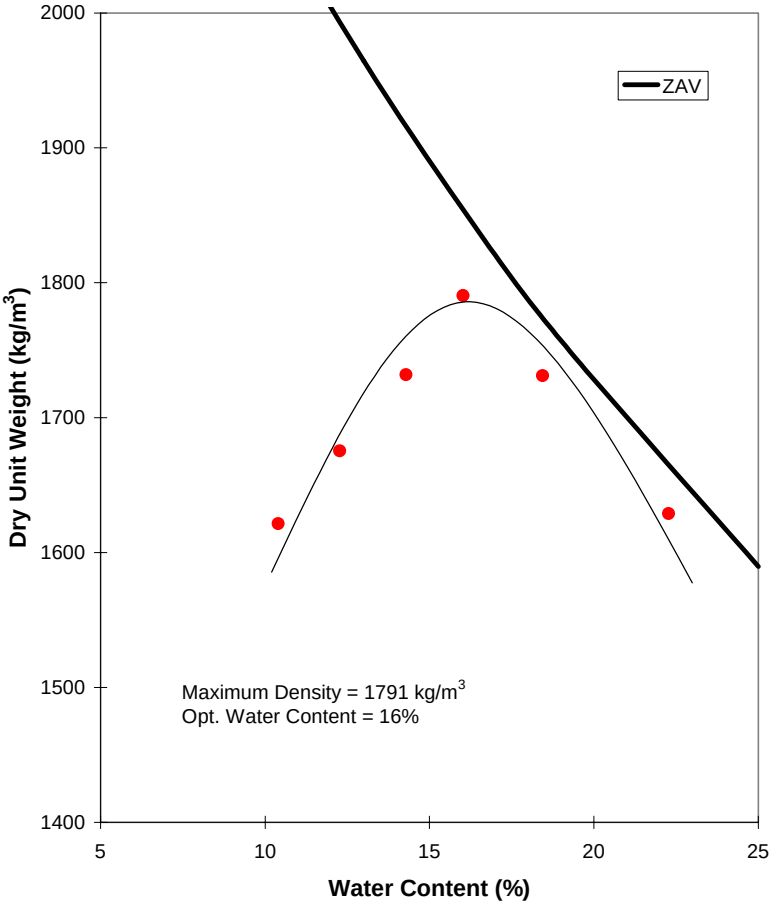

Figure 3. Moisture-Density relationship for A-6 subgrade soil

Table 1. Summary of classification test on the subgrade soil used in Test Section 708.

AASHTO	A-6
USCS	CL
Spec. Gravity	2.70
LL (%)	29
PI	13
Optimum moisture content (%)	16
Maximum Density (kg/m^3)	1791
% passing #10	99
% passing #200	92

The standard and modified moisture density relationships for the base material are presented in Figure 4 and maximum densities and optimum gravimetric moisture content are 2403 kg/m^3 (150 pcf), 2465 kg/m3 and 7.5%, respectively.

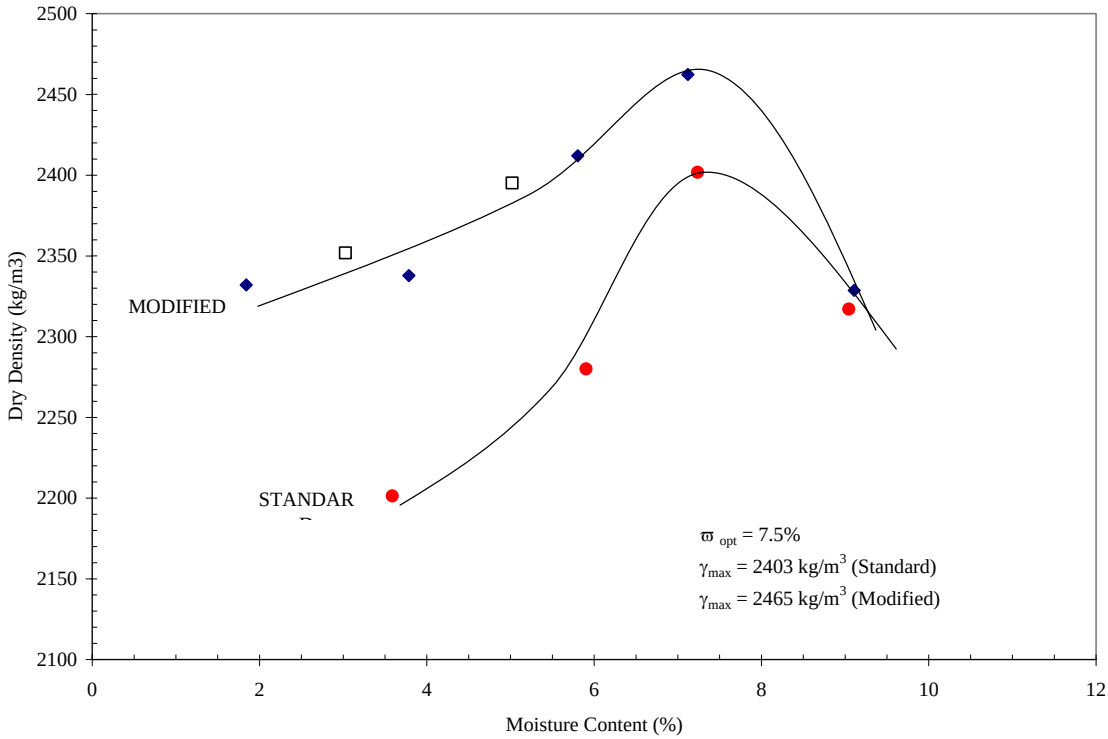

Figure 4. Moisture-density relationships for the base course soil.

The asphalt concrete material of the binder course conformed to the Vermont Type II standard, with 19-mm maximum aggregate particle size and 4.5% of asphalt binder PG-58-34. The asphalt concrete material of the wearing course conformed to the Vermont Type III standard, with 13-mm maximum aggregate particle size and 5.3% of asphalt binder PG-58-34. The nominal thickness of the binder course was 51 mm. The nominal thickness of the wearing course was 25 mm.

CONSTRUCTION OF THE TEST SECTION

The subgrade material from a previous test section (TS 706) was removed to a depth of 5 ft (1.52 m) from the AC surface. This material was then replaced in the new test section (TS 708) in 150-mm (6-in.) lifts. When the target moisture content was achieved, the exiting subgrade surface was roller compacted with two passes of a 10-ton (9072-kg) steel roller in static mode. Moisture and density quality control measurements were taken at every other subgrade soil layer, i.e., every 0.30 m (1 ft).

At the end of the test subgrade construction, the base course layer was placed in 2 layers of 114.3 mm (4.5 in.) thickness. Finally, the AC layer was placed in two lifts for a total of 76 mm (3 in.).

Construction Control

During the construction of the subgrade, a series of tests was conducted on the compacted layers. These measurements were conducted on every 300-mm lift unless otherwise noted. Measurements included layer thickness, which were taken with a survey level, and in-place TROXLER™ nuclear moisture/density measurements. A total of 360 measurements were taken in the subgrade layer and 42 were taken in the base and AC layers. Density measurements for the AC layer were taken; unfortunately, they were taken at the end of the accelerated pavement testing. Other measurements included elevation measurements on top of the subgrade, base, and AC layers and FWD tests on top of the completed test section.

The mean dry density of the subgrade was 1716 kg/m ^{3} (107.1 pcf) with a COV of 3%. For the base, the mean density was 2158 kg/m^3 (134.7 pcf) with a COV of 5.1%. The mean density of the AC was 142.6 pcf (2284 kg/m^3) with a COV of 2%. The mean moisture content of the test subgrade was 18.6% with a COV of 1.5 %. The average moisture content of the base was 4.0% with a COV of 15%.

The mean subgrade thickness was 132 in. with a COV of 0.2%. The mean base thickness was 8.9 in. with a COV of 4%. The mean AC thickness was 2.8 in. with a COV of 11%.

Instrumentation

Instruments for measuring stress, strain, temperature, and moisture content were installed in the pavement structure during construction of the test section. Details of the instrumentation can be found in Janoo et al. (2002). The locations of the gages in the test section were similar to those in Test Section 706.

Displacement measurements were made in the base and subgrade by means of εmu coils (Fig. 5). Strain can be deducted from displacement between a pair of coils. The sensors were placed 150 mm center to center. Displacements were measured in the longitudinal (x), transverse (y), and vertical (z) direction of loading. Displacements in the vertical direction were measured to a depth of 1.52 m.

Figure 5. Emu coils. A US 25-cent coin is included for scale reference.

A triaxial Dynatest® stress cell set was installed at a depth of 76 mm (3 in.) below the top of the subgrade in all test windows (Fig. 6). In Test Window 2 an additional triaxial stress cell set was installed at a depth of 229 mm (9 in.) below the top of the subgrade. The diameter of the Dynatest® stress cells was 76 mm (3 in.).

A triaxial Geokon® stress cell (Fig. 7) set was installed in the middle thickness of the base course in each of Test Windows 2 and 5. The diameter of the Geokon® stress cells was 229 mm (9 in.).

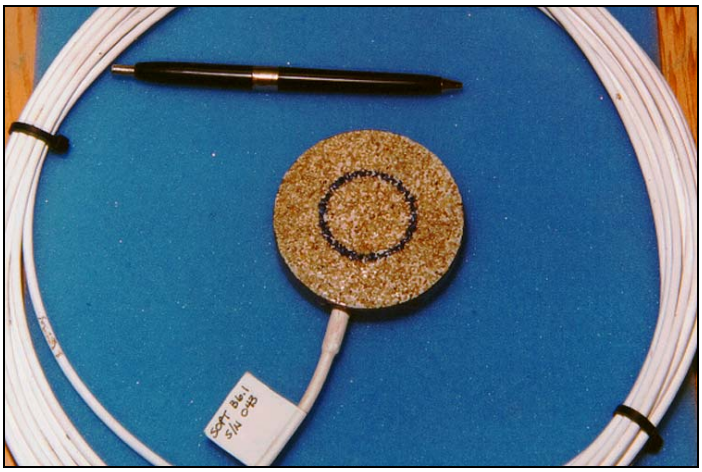

Figure 6. Dynatest® stress cell used in the subgrade.

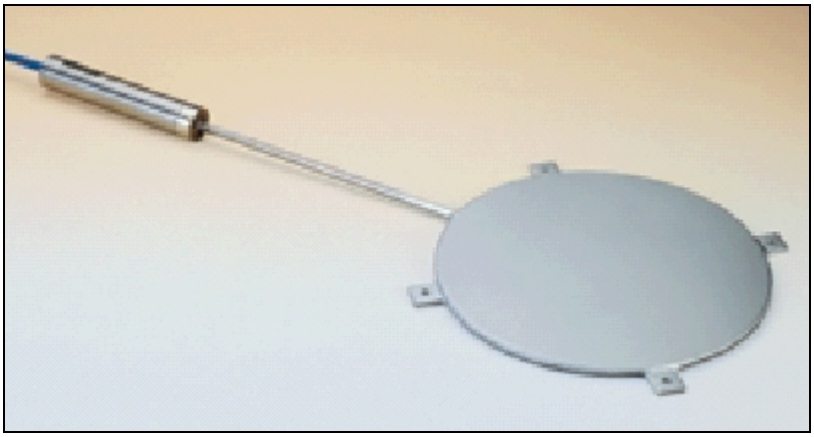

Figure 7. Geokon® stress cell used in the base course.

Soil moisture was measured with Vitel Hydra® soil moisture probes (Fig. 8). One set of two Vitel Hydra® soil moisture probes was installed in the subgrade at depths of 0.46 m (1.5 ft) and 0.76 m (2.5) from the top of the asphalt concrete at each of three representative locations in the test section. Through the use of appropriate calibration curves, the dielectric constant measurement was related to soil moisture. The Vitel Hydra® soil

moisture probes were calibrated for the AASHTO A-6 subgrade soil. Details on the calibration of the probes can be found in Janoo et al. (2002).

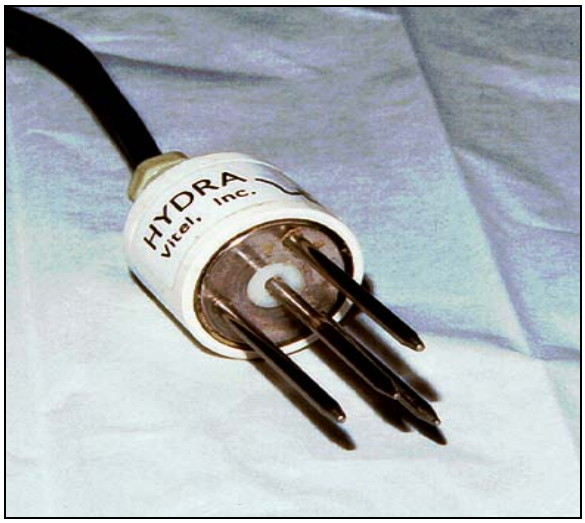

Figure 8. Vitel Hydra moisture sensor.

Subsurface temperatures were taken using thermocouple sensors. The thermocouples have an accuracy of ± 0.5°C. The subsurface temperature sensors were installed at three locations within the test section.

Testing Program

The test windows were subjected to accelerated traffic loads using CRREL's Heavy Vehicle Simulator (HVS). The following tests were conducted:

1. Prior to the accelerated load tests, FWD measurements on the surface of the AC layer using the same locations as during the construction phase.
2. Initial transverse profiles of each test window were measured using the 3-m-long laser profilometer (Fig. 9). The laser, located 45 cm from the ground surface, measured the surface profile at approximately 9-mm intervals.
3. In addition to the Profilometer measurements, level surveys were made during every test to determine whether the reference points (i.e., where the feet of the profilometer were located during the surface profile measurements) moved. The results from the level surveys indicated that the points were stationary throughout the test. Twenty transverse cross-section measurements spaced 0.3 m apart were made in each window (Fig. 10). Surface profile measurements were made at each traffic stop. The maximum rut depth was calculated as the difference of the surface profile after *N* passes to a baseline. The baseline was the measurement taken prior to loading of the test section. A typical surface rut measurement and the definition of maximum rut depth are shown in Figure 11. Testing was terminated when the average maximum surface rut depth of 12.5 mm was reached or exceeded.

Figure 9. Laser profilometer.

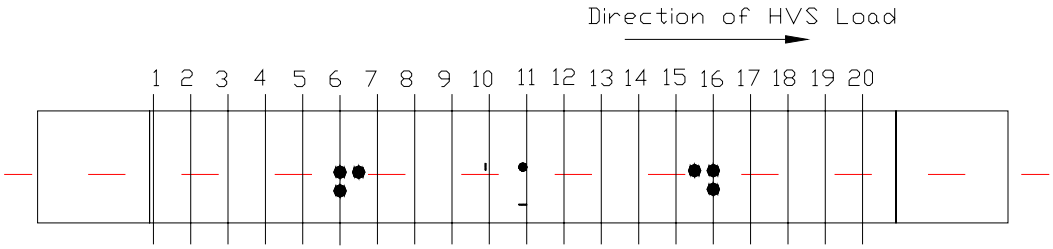

Figure 10. Locations for profile measurements in test section 708.

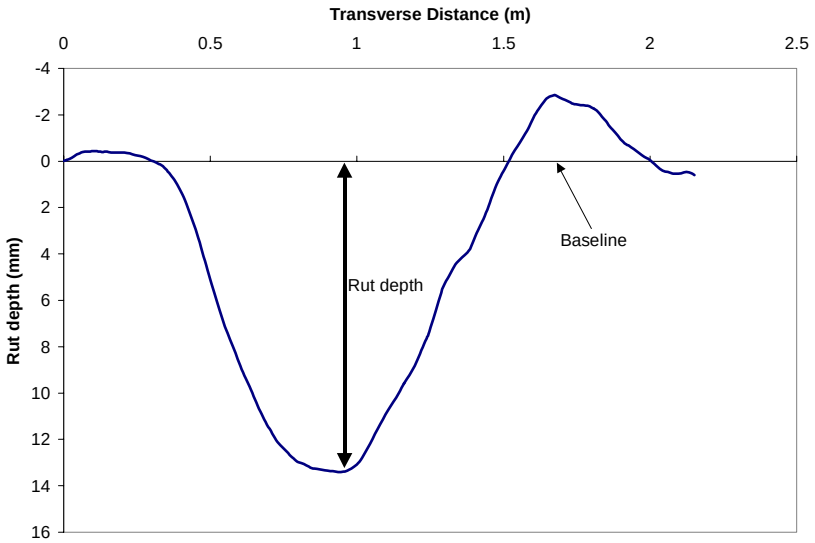

Figure 11. Definition of rut depth.

4. Subsurface stresses, strains, and permanent displacements were also measured in the vertical and in two perpendicular horizontal directions at several traffic-pass levels.

5. At the end of the dynamic stress-strain measurements, permanent deformation measurements were taken using the εmu coils (Fig. 12). A loose coil gage on the surface was used to measure the permanent deformation between the AC surface and the first coil in the base course.

Figure 12. Measuring displacement between the AC surface and the top of the base course.

SUMMARY OF RESULTS

Accelerated Traffic Loading

Traffic loading was applied by means of CRREL's Heavy Vehicle Simulator (HVS). The tire assembly was a dual-tire standard truck half axle. The traffic speed was 12 km/hr. The traffic was allowed to wander across the 1-m width. The mean applied loads are summarized in Table 2. The tire pressure was set to 690-kPa (100 psi).

Table 2. Mean load on test windows.

Test Window	Applied Load (kips)
708C1	9 (40)*
708C2	6 (27)
708C3	7 (31)
708C4	12 (53)
708C5	9 (40)
708C6	7 (31)

*Number in parenthesis is applied load in kilonewtons.

Table 3. Sequence of HVS tests on test windows

Window	Start	End	No. of test days
708C1	28-Apr-03	30-Apr-03	2
708C2	9-May-03	20-May-03	11
708C3	23-May-03	29-May-03	6
708C4	22-Apr-03	24-Apr-03	2
708C5	1-May-03	5-May-03	4
708C6	20-May-03	23-May-03	3

Moisture and Temperature

The mean air temperatures and the coefficient of variation (COV) in the test sections during the time of HVS testing are presented in Table 4. The subsurface temperatures fluctuated little around 19.5°C.

Table 4. Mean air temperatures during traffic testing of the test windows.

Test Window	Mean Temp (ºC)	COV
708C1	19.2	2.0
708C2	19.1	3.8
708C3	20.0	3.2
708C4	19.5	3.2
708C5	18.7	2.8
708C6	19.7	2.6

Moisture measurements in the subgrade taken during the testing period as a function of depth are presented in Table 5. The average is based on the previous 5 days before testing and during the testing period. At 18 in. (457 mm) from the top of the AC or 6 in. (150 mm) from the top of the subgrade, the average gravimetric moisture content was 19.9% with a COV of 5.1%. At about 30 in. (762 mm), the average moisture content was 17.1% with a COV of 8.1%. Overall, in the top 24 in. (610 mm), the average moisture content was 18.5% with a COV of 10%.

Table 5. Average moisture content in subgrade during HVS testing.

Depth (mm)	457	737	457	762	457	762
Test Window	Moisture Content (%)					
708C1	18.74	17.62	19.78	15.22	21.17	18.33
708C2	18.75	17.62	19.83	15.20	21.19	18.50
708C3	18.80	17.68	19.88	15.21	21.20	18.61
708C4	18.76	17.69	19.81	15.45	21.16	18.17
708C5	18.74	17.61	19.80	15.22	21.18	18.39
708C6	18.79	17.66	19.86	15.18	21.20	18.59

Similar measurements were made in the base course and the results are presented in Table 6. The average moisture content in the base course was 4.8% with a COV of 13%.

Table 6. Average moisture content in base course during HVS testing.

Depth (mm)	152	152	152
Test Window	Moisture Content (%)		
708C1	4.14	4.49	5.68
708C2	4.20	4.53	5.57
708C3	4.21	4.54	5.56
708C4	4.13	4.51	5.59
708C5	4.17	4.50	5.65
708C6	4.22	4.55	5.56

Surface Rut Measurements

Transverse surface profile measurements were taken periodically during testing. The rut depth was calculated as the difference between the profile measurements taken at the pass level and the profile measurements taken prior to testing. Profile measurements were taken every 305 mm, starting from one end of the test window (within the constant speed zone), for a total of 20 locations.

The maximum rut depths from transverse profile measurements were used to develop the longitudinal profile. The longitudinal rut depth in various test windows as a function of load repetitions are presented in Figure 13. First, it can be seen that it did not take many passes to exceed a surface rut of 12.5 mm (1/2 in.). Second, the longitudinal ruts are fairly uniform across the test window.

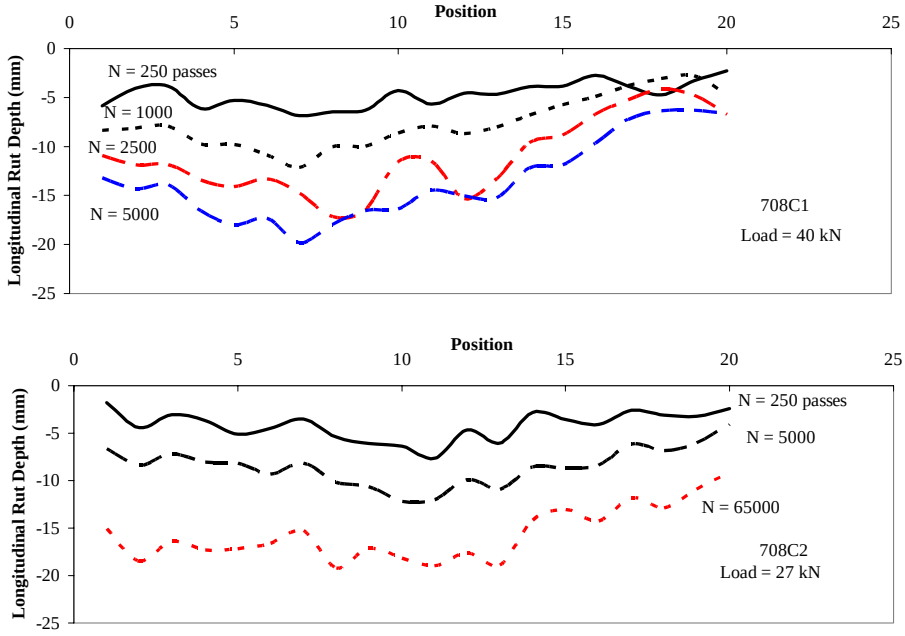

a. In TS708C1 and TS708C2.

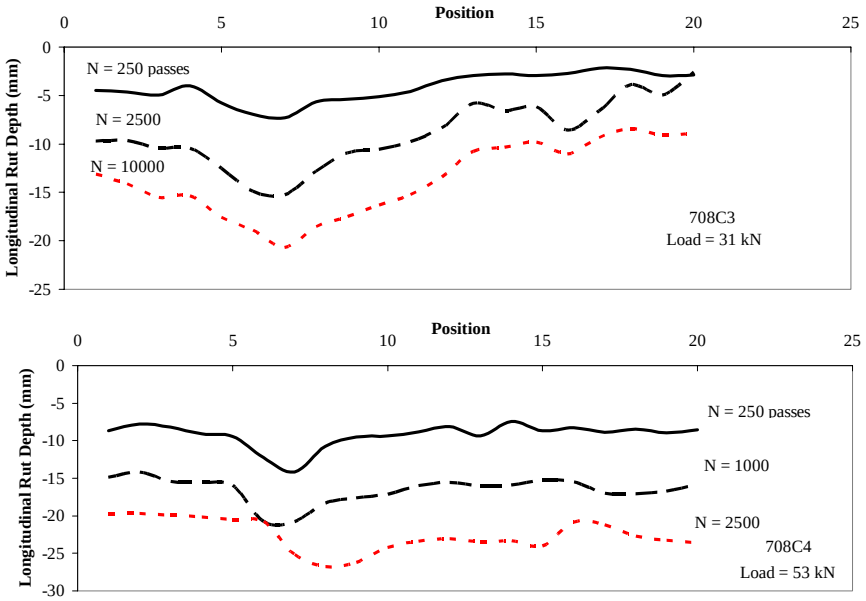

b. In TS708C3 and TS708C4.

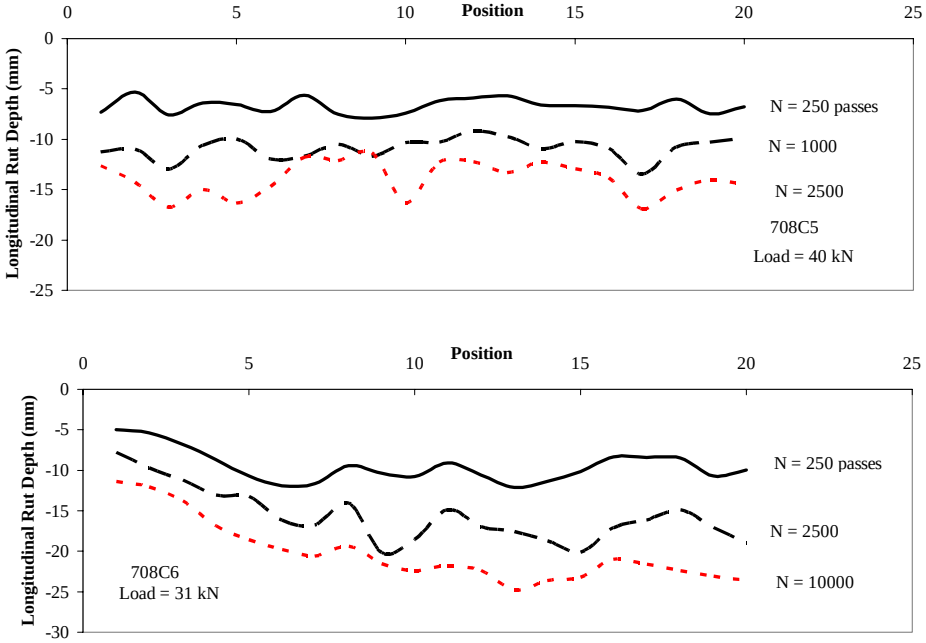

c. In TS708C5 and TS708C6.

Figure 13. Longitudinal rut formation.

The progressions of rut depths as a function of load repetitions in the various windows are presented in Figure 14. In general, as the applied load increased so did the rate of rut depth.

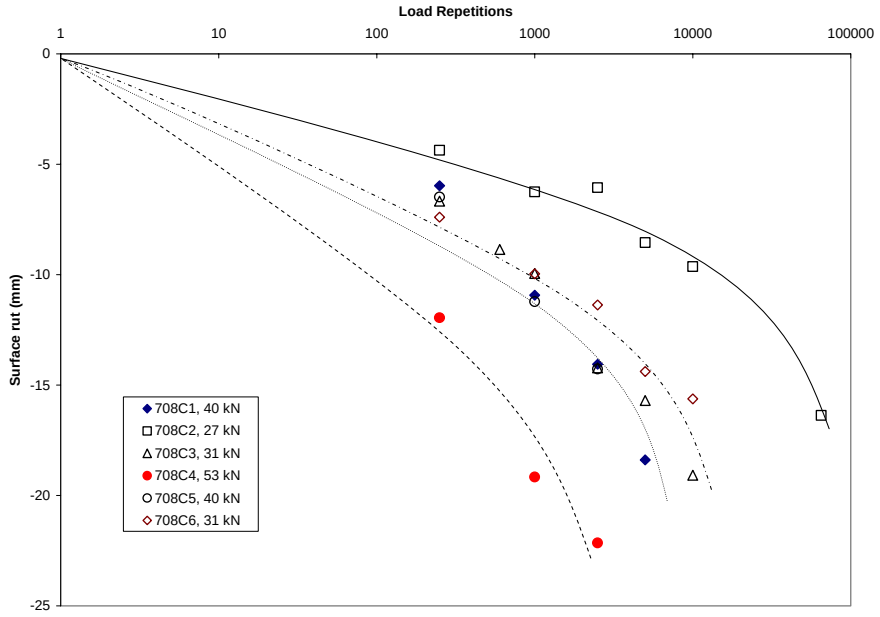

Figure 14. Rut depth progression as function of load repetitions.

The data from the surface profile measurements were also used to estimate the number of load repetitions required to reach failure. Failure was defined when the average rut depth reached a 12.5 mm. The estimated load repetitions were then used with the appropriate power equations to estimate the failure stresses and strains (Table 7).

Table 7. Load Repetitions to reach failure of 12.5-mm.

Test Window	Passes to failure
708C1	1703
708C2	24791
708C3	2079
708C4	278
708C5	1559
708C6	3155

Strain Measurements

Permanent deformations and strains

Permanent deformation and strain measurements were collected in the base and subgrade. During the test, a surface coil and the coil under the AC layer are used to determine the deformation of the asphalt layer with increasing load application.

The vertical permanent deformations on the top of the subgrade as a function of load repetitions are shown in Figure 15. The deformations were compressive and there appears

to be correlation between applied load and permanent deformation with the exception of 708C3 and 708C6 (not shown in Fig. 15). Cortez reported that prior to the testing of 708C6, he found that the surface of the pavement showed an upheaval. This he thought was from the rutting in 708C2. A similar situation may have happened to 708C3. Although shown in Figure 15, the permanent deformation in 708C3 and 708C6 were not used in any future analysis. Power curves were fitted to the strain data (combined the results from 708C1 and 708C5) and the results are presented in Figure 16 and in Table 8.

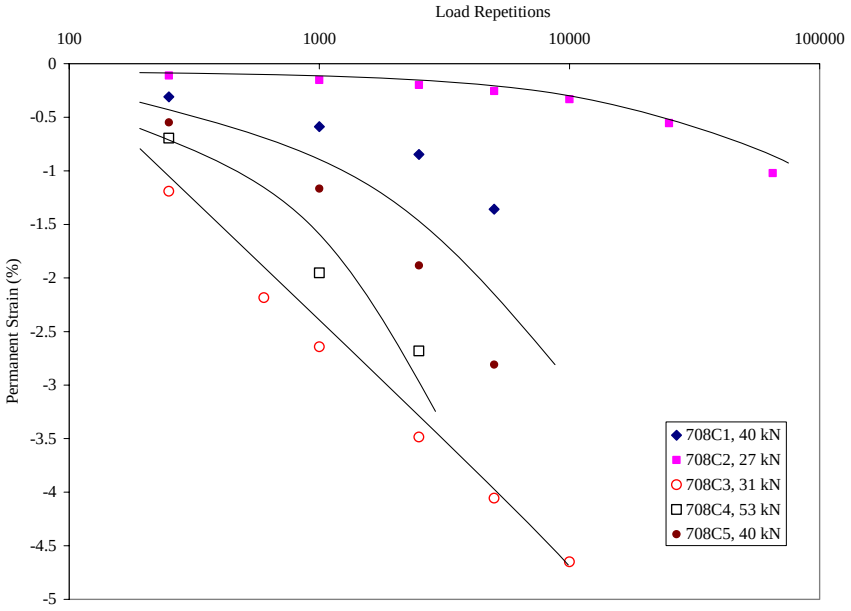

Figure 15. Permanent strains at 76 mm below the top of subgrade layer.

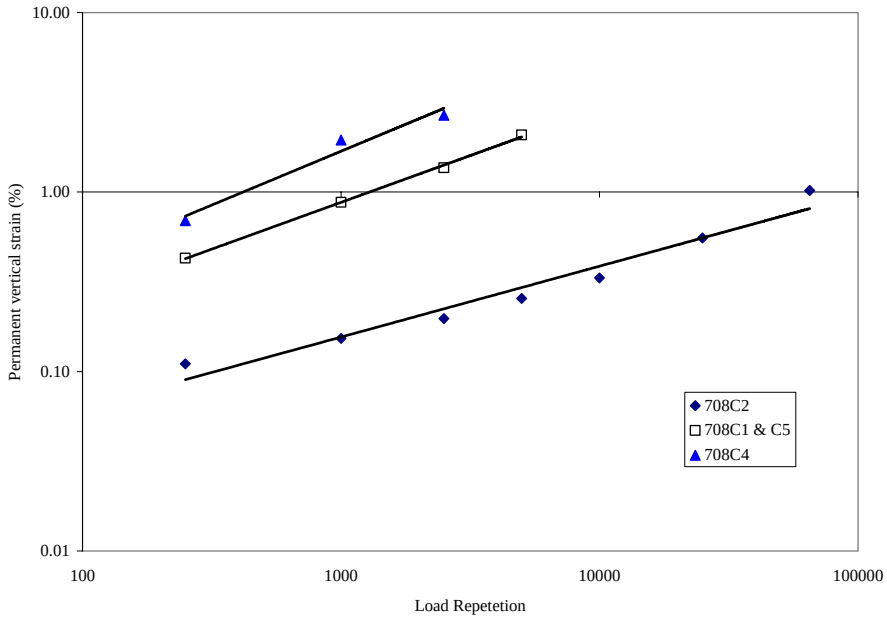

Figure 16. Permanent strains at 76 mm below the top of subgrade layer as a function of load repetitions

Table 8. Power curve coefficients for the vertical permanent strains (%).

Test Window	Load (kN)	*A*	*n*	R^2
708C1 & C5	40	0.0102	0.3948	0.96
708C2	27	0.0239	0.5215	0.99
708C4	53	0.0267	0.6001	0.97

Dynamic Displacements and Strains

As with previous test sections, triaxial dynamic displacements were measured with the εmu coil gages in the base and subgrade. The vertical displacements were compressive, whereas the peak longitudinal and transverse displacements were tensile. In general, the greater the load, the greater was the displacement. The change in vertical strain as a function of load repetition is presented in Figure 17. Power curves were fitted to the data and the coefficients are presented in Table 9.

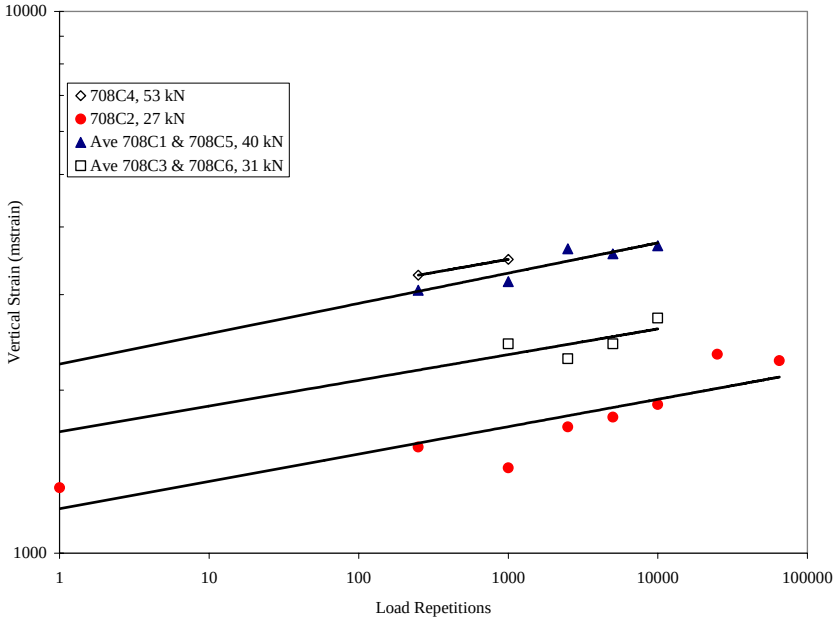

Figure 17. Peak dynamic vertical strains of subgrade as function of load repetitions

Table 9. Power curve coefficients for the vertical strains.

Test Windows	Load (kN)	*A*	*n*	R^2
C1,C5	40	2235	0.0559	0.86
C2	27	1208	0.0505	0.76
C3, C6	31	1675	0.0475	0.42
C4	53	2491	0.0487	

Stress Measurements

Triaxial stress measurements were made in the subgrade in all test windows at an approximate depth of 380 mm from the pavement surface, with the exception of 708C6. In TS708C2 and 708C5, an additional set of triaxial stress measurements was made at 533 mm from the AC surface. All stress measurements were compressive.

During testing it was found that the stress cells were located approximately within 1 ft of the centerline where it was normally placed. This discovery was found after the tests were completed. A series of stress tests were conducted at the centerline, 203 mm (east of centerline), 152, 356, 559, and 1219 mm (west of centerline) to determine the maximum stress and therefore the multiplication factor that needed to be applied to all the stress measurements. The results from the tests are shown in Figure 18. Based on the test results, we increased the measured vertical stress by 20%, the longitudinal stress by 9%, and the transverse stress by 4%.

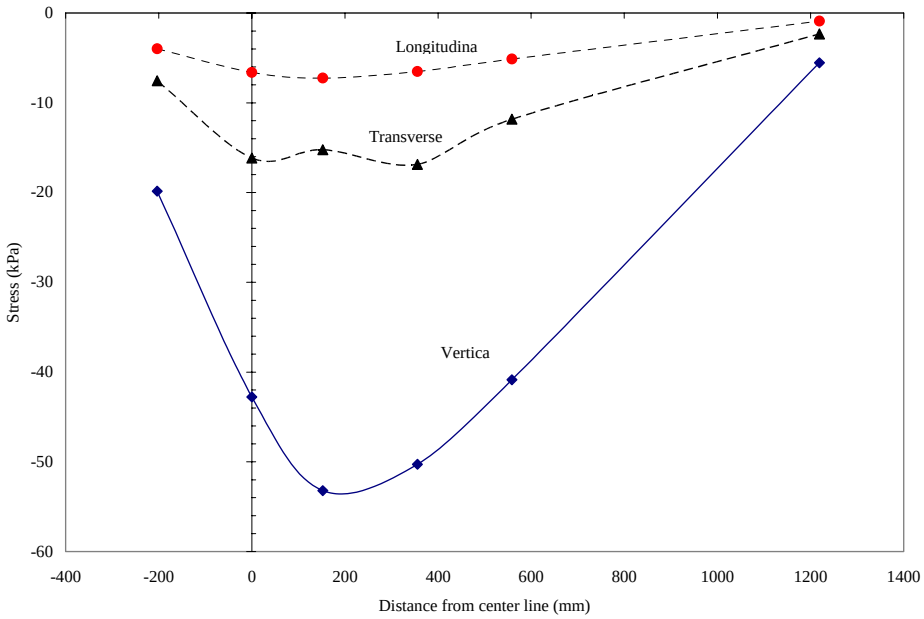

Figure 18. Influence of lateral wander on stress measurements

The changes in stress at a depth of 381 mm (15 in.) from the AC surface as a function of load repetitions are presented in Figure 19. Generally, we do see a decrease in the stress with increasing load repetitions. This is more apparent at higher load levels. With the exception of the load at 53 kN, the change in stress is small at 40 kN and below.

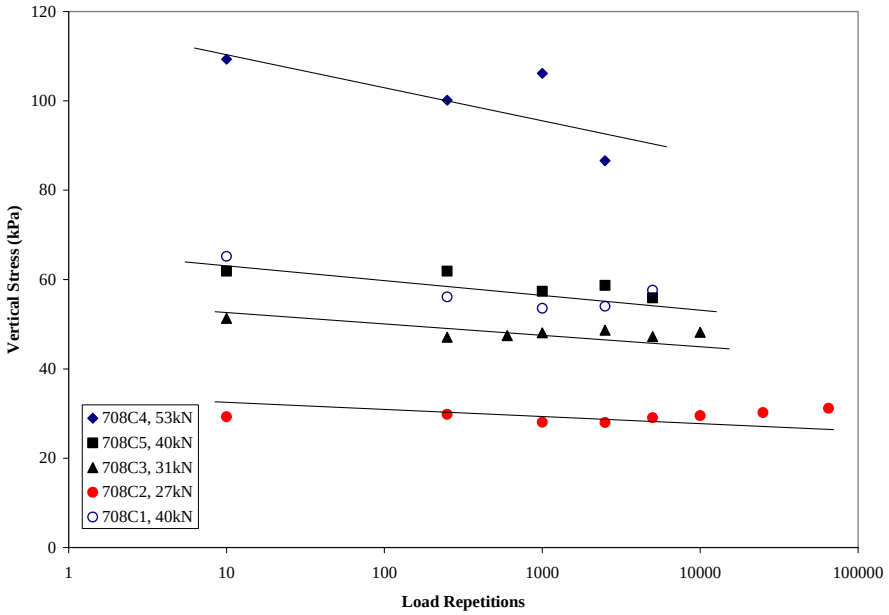

Figure 19. Influence of applied load on stress measurements at depth of 381 mm from the top of the AC layer.

FORENSIC EVALUATION

As shown in the cover of this report, the research plan includes a test section for each of four subgrade soil types, each at three subgrade moisture contents. One of the moisture contents is the optimum. Another test section is built as wet as it can be reasonably built, and a third test section is build with an intermediate moisture content.

Test Section 708 was built with a subgrade soil AASHTO type A-6 conditioned to be at nominal 19% gravimetric moisture content during construction. Test Section 706 was built with the subgrade soil conditioned at nominal 22%. Test Section 709 was built with the subgrade soil conditioned at optimum moisture content of 16%.

A forensic exploration was conducted to establish the condition of the pavement structure at the end of the traffic tests (Fig. 20 and 21).

One trench was excavated across test windows 1, 2, and 3 on the south region of the test section. This trench will be referred to as the “South Trench.” Another trench was excavated in the north region of the test section. This trench cuts across test windows 4, 5, and 6. The trenches had to be carefully located to avoid damaging the embedded sensors.

The areas of the trenches were marked with paint over the asphalt pavement. A dry saw was used to neatly cut the asphalt concrete layers so that reliable layer thickness measurements could be made. Rod and level elevation measurements were taken at 0.20-m (8-in.) spacing along the edge of the trenches.

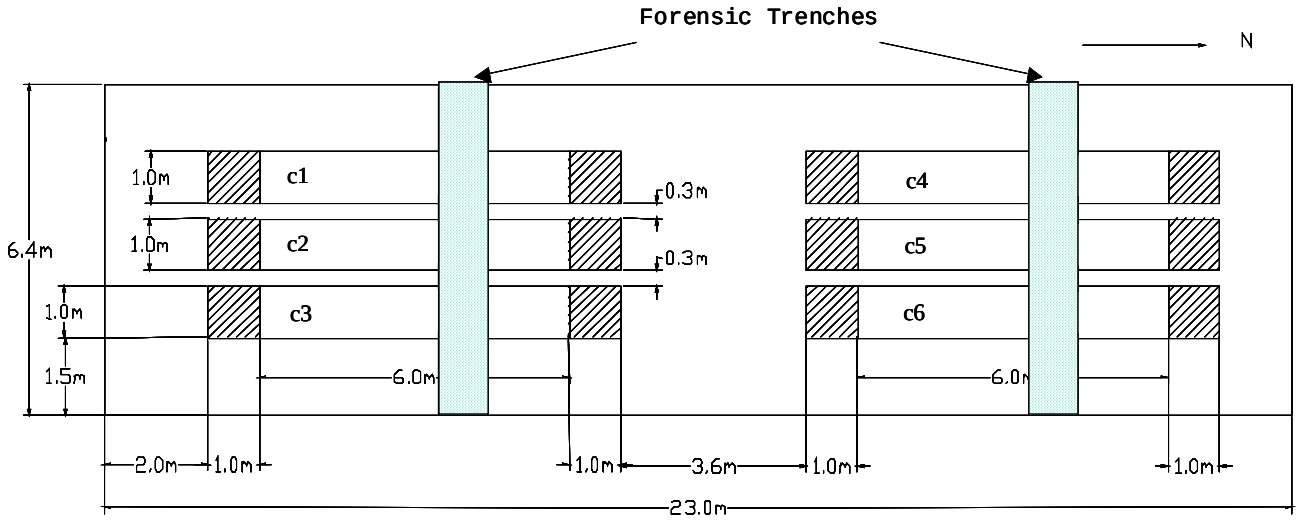

Figure 20. Location of the forensic trenches in Test Section 710.

Figure 21. Forensic trench.

As soon as the asphalt layer was removed from the trenches, base course samples were collected at 0.20-m (8-in) spacing along one side of the trenches. These samples were used to determine moisture content by the oven-dry method.

Sand cone measurements were conducted in the base course in the trench areas (Fig. 22–24). One test location represented the center of the tire path for each test window. In addition, sand cone measurements were conducted outside the test windows.

Figure 22. Sand cone density measurements in the base course.

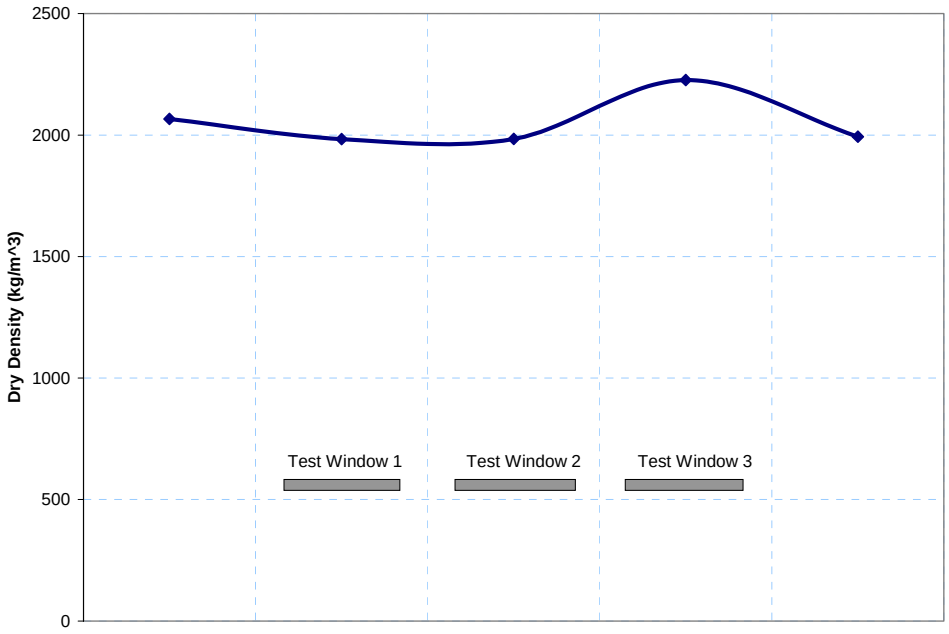

Figure 23. Base course density measured by the sand cone method in the south trench.

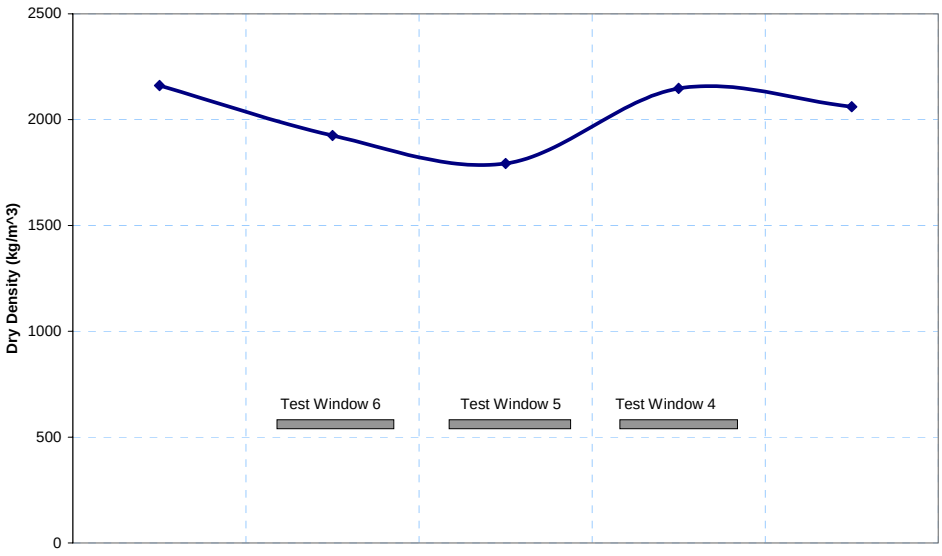

Figure 24. Base course density measured by the sand cone method in the north trench.

Vane shear tests were conducted at various depths in the subgrade at 33 locations along each trench (Fig. 25–27).

Figure 25. Vane shear measurement in the subgrade.

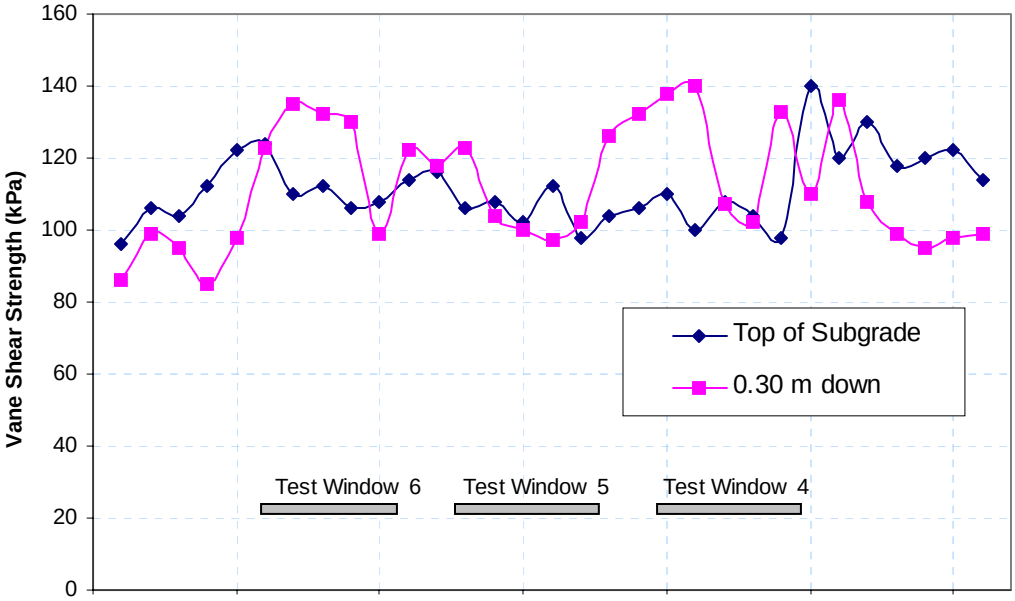

Figure 26. Vane shear strength measurements in the south trench across Test Windows 1, 2, and 3.

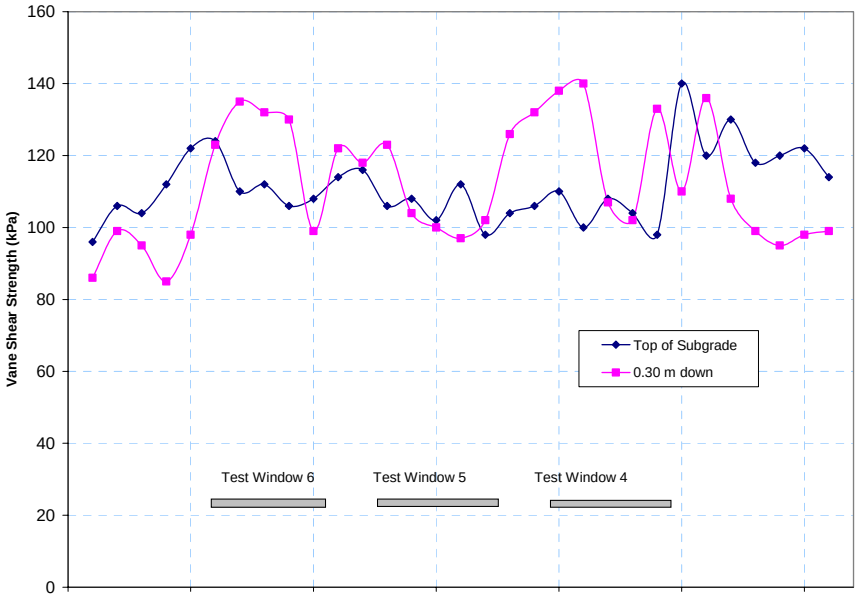

Figure 27. Vane shear strength measurements in the north trench acrossTest Windows 4, 5, and 6.

Nuclear moisture and density measurements were taken in the trenches at each layer. The measurements were conducted in the direct mode, i.e., the probe was inserted 0.15 m (6 in.) into the soil. The measurement represents the region of soil between the inserted nuclear source and the receiver in the box of the apparatus. Drive cylinder tests samples

were taken in the same volume where the nuclear gauge measurements were taken (Fig. 28–30).

Figure 28. Nuclear gauge density measurement in a trench.

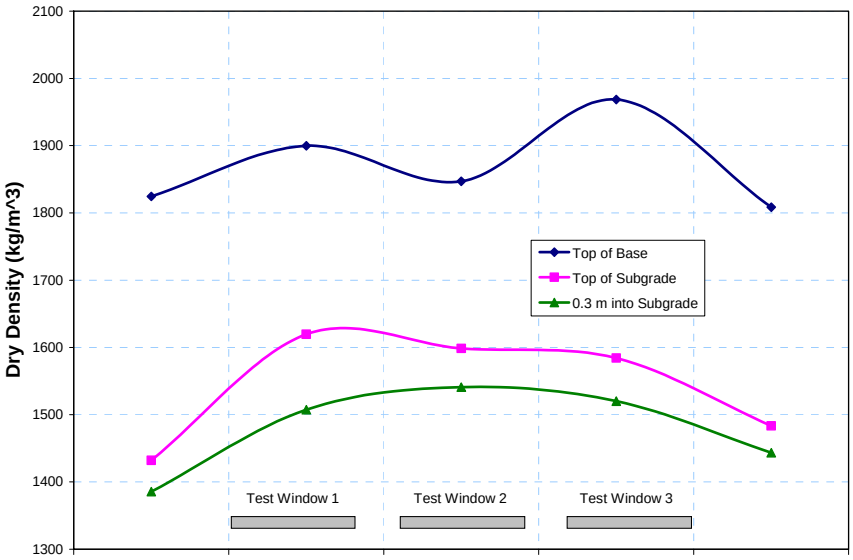

Figure 29. Soil densities in the base course and in the upper subgrade in Test Windows 1, 2, and 3,and at the sides of the test windows.

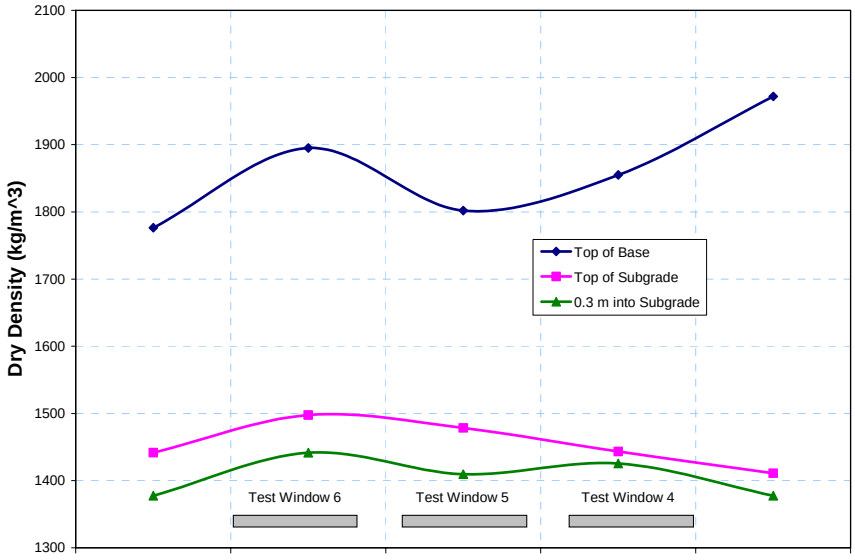

Figure 30. Soil densities in the base course and in the subgrade in Test Windows 4, 5, and 6, and at the sides of the test windows.

A portable falling weight deflectometer was used to measure the composite soil modulus at various layers in the subgrade at the trenches (Fig. 31–33).

Figure 31. Portable falling-weight deflectometer measurements in the trenches.

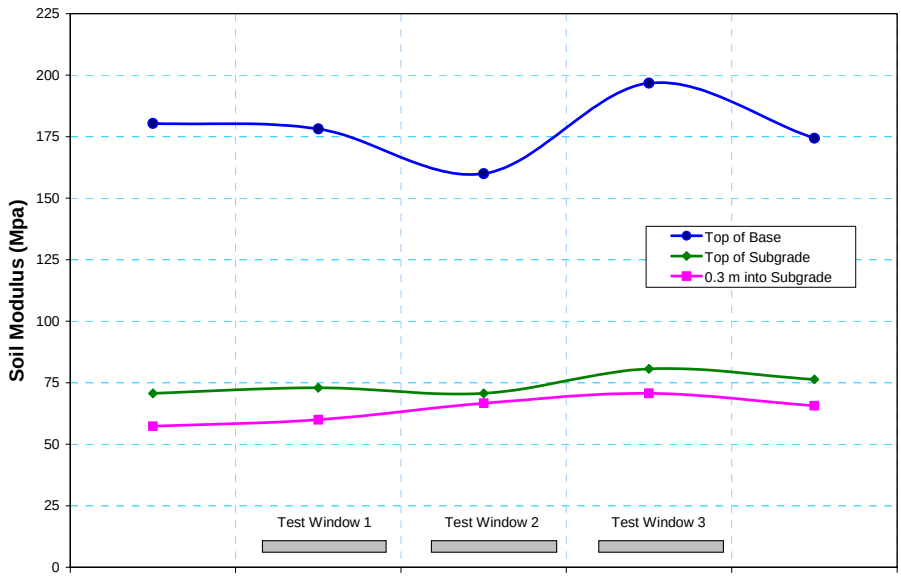

Figure 32. Soil modulus measured with the portable falling-weight deflectometer in the south trench.

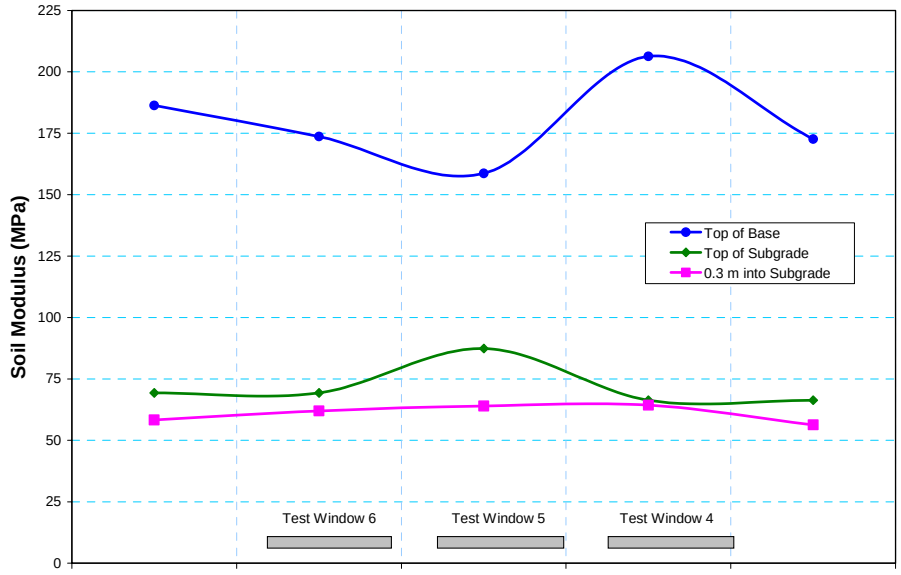

Figure 33. Soil modulus as measured with the portable falling-weight deflectometer in the north trench.

Dynamic Cone Penetrometer (DCP) measurements were conducted in the trenches at each test window inside and outside the traffic area. DCP tests were initiated on the top of the subgrade, and at 0.30- and 0.60-m depths into the subgrade. The DCP measurements were correlated to California Bearing Ratio (CBR) values (Fig. 34–36).

The DCP readings were correlated to CBR values by the equation:

$$\text{Log CBR} = 2.46 - 1.12 \times \log \text{DCP} \quad (1)$$

where DCP is in mm/blow.

This correlation was developed at the US Army Corps of Engineers Waterways Experiment Station (WES). WES developed the above correlation based on testing of a variety of soils. The DCP test apparatus used at CRREL was manufactured by Kessler Soils Engineering Products, Inc.* The DCP–CBR conversions were obtained using an automated Excel spreadsheet provided by the instrument manufacturer. The spreadsheet implements the CBR–DCP correlations developed by WES.

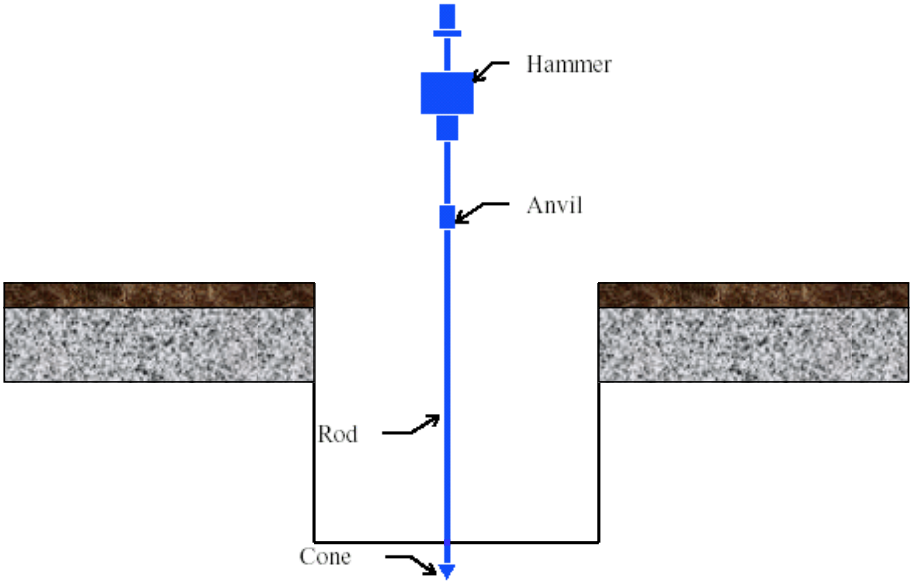

Figure 34. Dynamic cone penetrometer measurements in the trenches.

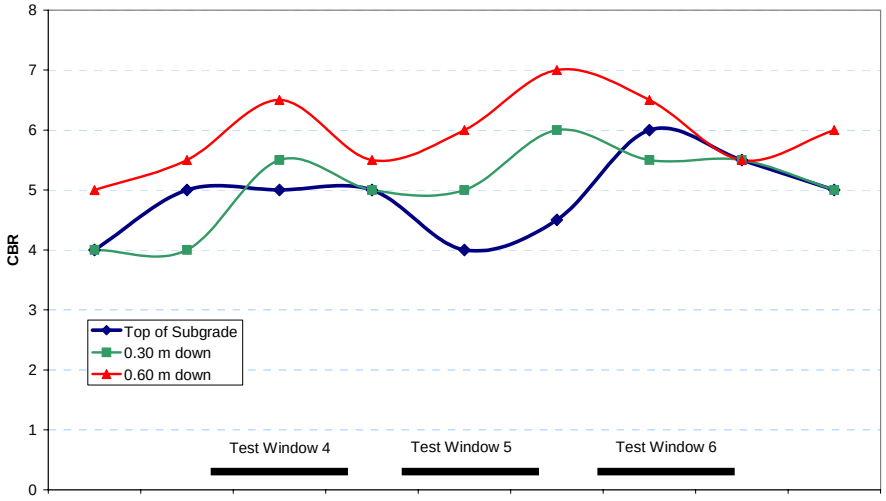

Figure 35. CBR values obtained from DCP measurements in the south trench.

* http://www.kesslerdcp.com/info.html

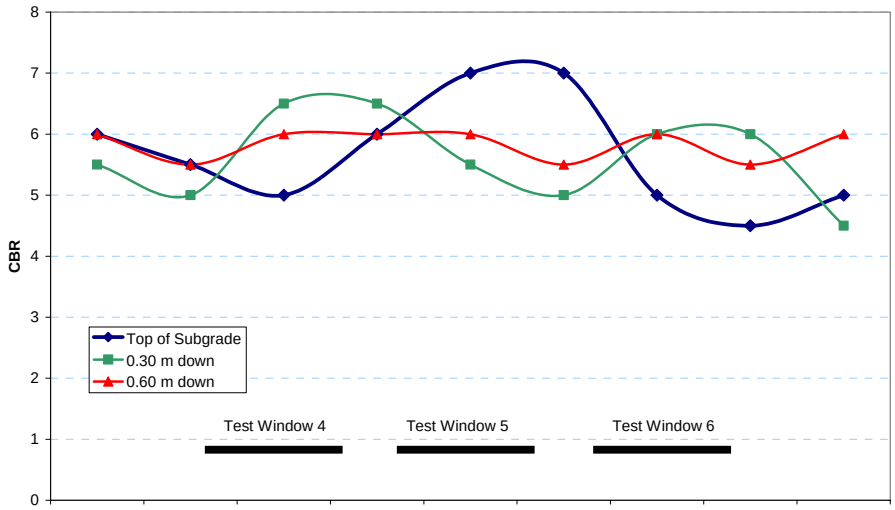

Figure 36. CBR values obtained from DCP measurements in the north trench.

When the trenches were completed, one wall of the trench was carefully cleaned to be able to measure the actual thickness of the asphalt concrete and the base course at the end of the traffic tests (Table 10).

Table 10. Thickness (mm) of asphalt and base course layers.

Test Window	Under Wheel Path		Outside of Test Window	
	AC	Base Course	AC	Base Course
1	64	269	70	270
2	70	267	70	270
3	62	271	64	267
4	95	258	89	257
5	94	262	89	264
6	62	264	73	248
Average	75	265	76	262

Oven dry moisture tests were conducted on samples taken from the base. The oven dry moisture test results are presented in Figures 37 and 38.

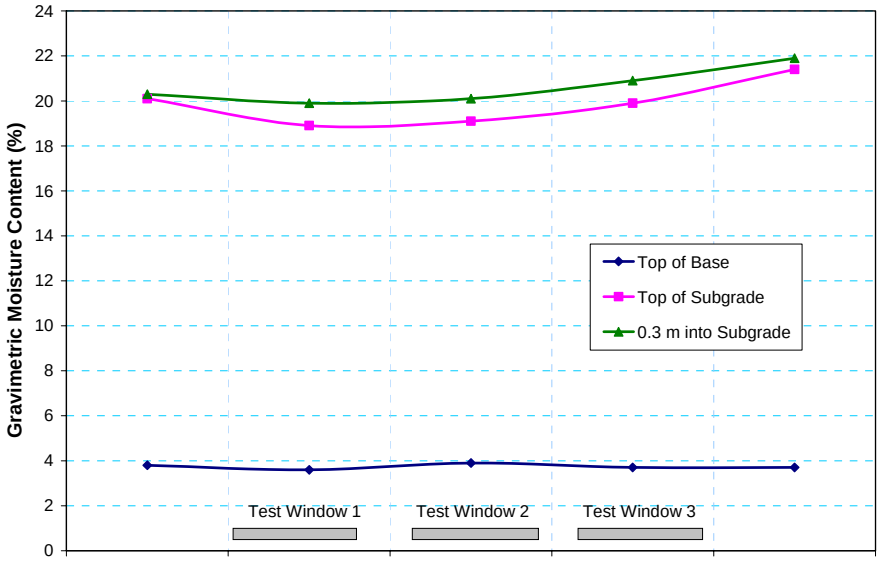

Figure 37. Gravimetric moisture content in the base course and subgrade in the north trench.

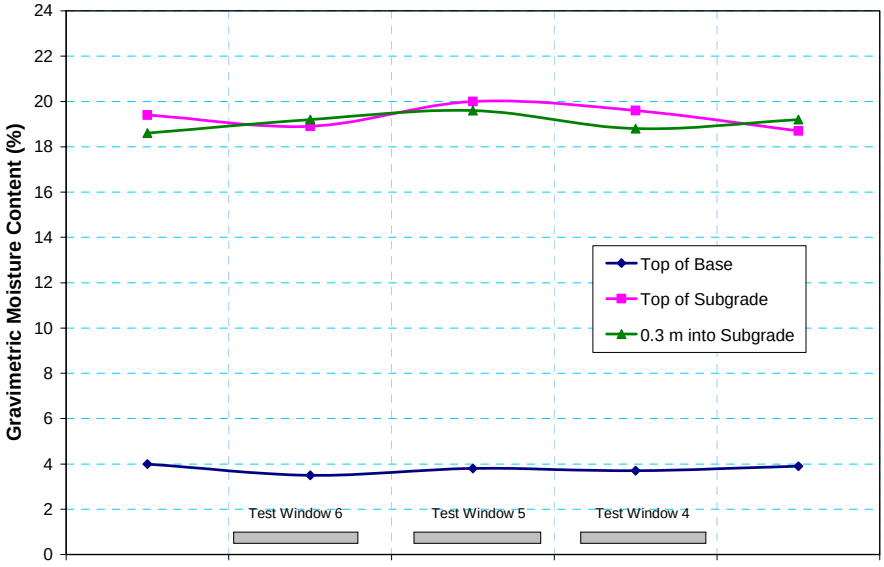

Figure 38. Gravimetric moisture content in the base course and subgrade in the north trench.

FORENSIC OBSERVATIONS

The surface rutting and overall response of the pavement in this test section was as expected. The only exception was an increased surface rutting observed at the north end

of Test Window 708c6. However, the forensic test results did not detected any difference in the measured parameters that could explain this behavior.

The moisture content measurements obtained during the forensic exploration indicate that there was no measurable loss of moisture in the subgrade during the traffic loading period. However, the moisture content in the base course decreased slightly during this period.

The asphalt thickness measurements taken on one side of the trenches show no difference between the traffic areas and the areas outside the test windows.

SUMMARY AND CONCLUSIONS

Accelerated pavement testing was conducted on a test section with an AASHTO type A-6 subgrade soil placed at wet of optimum density and moisture content of 1716 kg/m^3 and 19%, respectively. The subgrade layer was instrumented with stress, strain, temperature and moisture sensors.

The test section was divided into 6 test windows and accelerated pavement testing was conducted over a period of 1 month. During the accelerated pavement testing, dynamic stresses, dynamic and permanent strains, and surface rut depth measurements were collected at given loading intervals. Stress measurements were collected in all of the six test windows. Strain measurements were collected in all six windows to a depth of 1.2 m into the subgrade. Stress and strain measurements were made in the vertical, longitudinal, and transverse directions of loading. Temperature and moisture measurements were made every 4 hours during the tests. The test loads varied between 27 to 53 kN. The average tire pressure was 690 kPa.

The dynamic strains at failure are compared with the current Asphalt Institute and Shell subgrade failure criterions (Fig. 39). In additions the strains at failure from the other subgrades are shown in Figure 39. Note that these results were measured at 12 km/hr. To be able to compare with the results from the AASHTO Road tests, where the test speed was 48 km/hr, a correction factor was applied to the strain data. The correction factors were developed based on results from MnRoad (Dai and Van Deusen 1998, Janoo et al. 2002). The test results were multiplied by factors of 0.63 and 0.48 for speeds of 48 km/hour (AASHTO Road Test) and 88 km/hour (highway) respectively.

In terms of the allowable number of load repetitions N_d to limit rutting on top of the subgrade,

$$N_d = f_4 \left(\varepsilon_v\right)^{-f_5} \tag{2}$$

where the coefficients f_4 and f_5 are 0.0122 and –1.8454 for highway speeds.

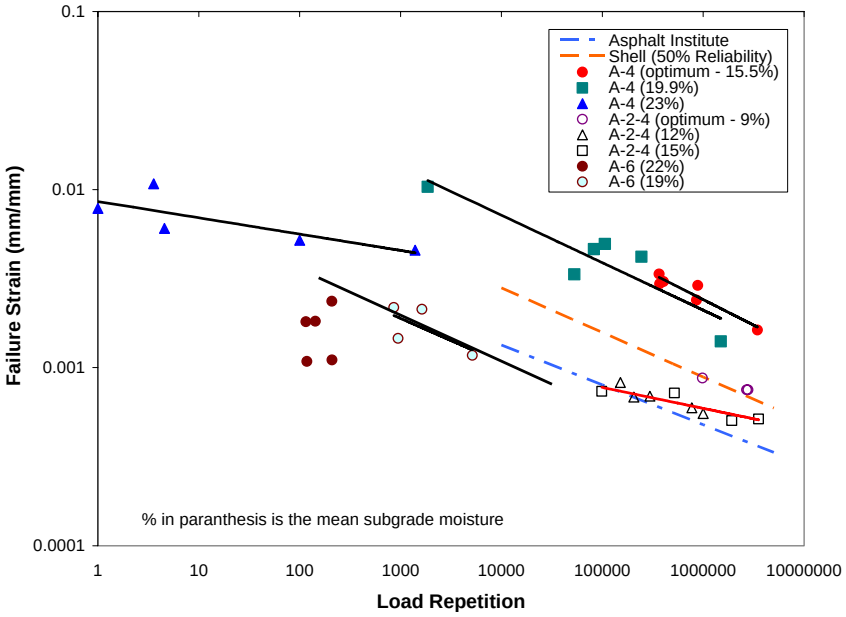

Figure 39. Effect of soil type on the subgrade failure criterion.

REFERENCES

Dai, S.T., D.Van Deusen, D.Rettner and G.Cochran (1997)Investigation of Flexible Pavement Response to Truck Speed and FWD Load Through Instrumented Pavements, *Proceedings of the 8th International Conference on Flexible Pavements. Seattle, Washington*, pp.141–160.

Hilderbrand & Irwin (1994) Theoretical Analysis of Pavement Test Sections in the FERF, Internal Report.

Janoo, V., L. Irwin, R. Eaton, and R. Haehnel (2001)Pavement Subgrade Performance Study: Project Overview, ERDC/CRREL Technical Report TR15, in prep.

Janoo, V., E. Cortez, and R. Eaton (2002) Pavement Subgrade Performance Study, A-2-4 Test Soil at Near Optimum Conditions, ERDC/CRREL Technical Report TR53, in final prep.

Janoo, V., E. Cortez, and R. Eaton (2002) Pavement Subgrade Performance Study, A-2-4 Test Soil at Wet of Optimum, ERDC/CRREL Technical Report TR54, in final prep.